



# Carbon–vacancy interaction controls lattice damage recovery in iron

D. Terentyev,<sup>a,\*</sup> K. Heinola,<sup>b</sup> A. Bakaev<sup>c</sup> and E.E. Zhurkin<sup>d</sup>

<sup>a</sup>*SCK•CEN, Nuclear Materials Science Institute, Boeretang 200, Mol B2400, Belgium*

<sup>b</sup>*Department of Physics, University of Helsinki, PO Box 43, FIN-00014 Helsinki, Finland*

<sup>c</sup>*Center for Molecular Modeling, Department of Physics and Astronomy, Ghent University, Technologiepark 903, 9052 Zwijnaarde, Belgium*

<sup>d</sup>*Department of Experimental Nuclear Physics K-89, Institute of Physics, Nanotechnology and Telecommunications, St Petersburg State Polytechnical University, 29 Polytekhnicheskaya Str., 195251 St Petersburg, Russia*

Received 5 March 2014; revised 7 April 2014; accepted 8 April 2014

Available online 16 April 2014

Ab initio techniques are applied to assess the positron lifetime of carbon–vacancy (C–V) complexes in iron for the first time. Positron lifetime is extremely sensitive to C–V arrangement and multiplicity. Following the ab initio lifetime data, a C–V complex can be detected as a single or clustered vacancy, or remain indistinguishable from bulk. Combining ab initio data with kinetic rate theory, we modelled annealing of irradiated Fe–C alloys and performed one-to-one comparison with experiment, which revealed a good agreement.

© 2014 Acta Materialia Inc. Published by Elsevier Ltd. All rights reserved.

**Keywords:** Iron; Interstitial carbon; Lattice damage; Recovery; Annealing

The radiation resistance of crystalline materials is determined by their ability to recover lattice defects produced by energetic particles. The addition of impurities is crucial from the metallurgical viewpoint, while their presence usually has a tremendous effect on the recovery of lattice defects. The most common example is iron–carbon (Fe–C) solid solution representing the matrix for steels currently operating and being proposed for future nuclear concepts [1]. C atoms affect mechanical properties before and after irradiation, implying their interaction with both dislocations and radiation-induced lattice defects. In-depth experimental investigations discovered that C atoms strongly bind to vacancies (V) and weakly with self-interstitial atoms (SIAs) [2,3]. C atoms therefore “glue” vacancies in clusters and hinder their migration, provoking nucleation of nanovoids. Consequently, carbon–vacancy (C–V) interaction plays a crucial role in the process of accumulation and recovery of radiation damage macroscopically seen as

hardening, swelling and creep under prolonged irradiation.

Although significant experimental [2,3] and theoretical [4–7] efforts have been dedicated to unravelling the interaction of C with radiation defects, the annealing of irradiated Fe–C alloys in the technological temperature range is not yet completely understood [8,9]. A combination of resistivity measurements (RMs) and positron annihilation spectroscopy (PAS) is the standard way to investigate the elementary recovery processes driven by the migration of radiation-induced defects [10]. Both RM and PAS techniques reveal that complete recovery of vacancies in Fe–C alloys occurs around 600 K [2,3]. This temperature corresponds to the energetic stability of double carbon–vacancy (2CV) clusters, whose dissociation energy is  $\sim 1.8$  eV [5].

If the initial concentration of vacancies,  $C_V$ , exceeds the amount of dissolved C atoms,  $C_C$ , then damage annealing is controlled by clustering of vacancies and their subsequent evaporation. In the opposite case (i.e.  $C_C > C_V$ ), the formation of C–V clusters leads to a complex positron annihilation spectrum, revealing both isolated and clustered vacancies at 450–600 K [3].

\* Corresponding author. Tel.: +32 14333197.; e-mail: [dterenty@sckcen.be](mailto:dterenty@sckcen.be)

A recent analysis employing ab initio data on the stability of C–V complexes and kinetic Monte Carlo (kMC) simulations [8] reported disagreement with experimental data in the temperature range 450–600 K. While vacancy clustering took place experimentally [3], it could not be reproduced in the simulations [8]. Moreover, even the interpretation of PAS data and direct comparison with kMC calculations is challenging since carbon significantly alters the lifetime of a positron trapped by C–V complexes [11,12]. Although several PAS studies have been performed on electron- and neutron-irradiated Fe and Fe–C alloys [13,14], the lifetime of multiple C–V complexes cannot be decomposed from the experimental spectra. Consequently, information on the structure of C–V complexes appearing in the technological temperature range remains unknown, while this is a crucial input for coarse-grain models dealing with the evolution of radiation damage and its recovery in Fe–C alloys.

Here, we employed density functional theory (DFT) to assess the thermal stability and positron lifetime of C–V complexes in body-centered cubic (bcc) Fe. Confronting the obtained lifetime against the experimental data allowed physically plausible assumption on mobility of the 2CV cluster to be made, which is necessary to complete the formulation of a self-consistent model describing the evolution of both isolated and clustered vacancies upon irradiation and subsequent annealing. As proof, we employed kinetic rate theory calculations to model annealing of electron-irradiated Fe–C alloys using the DFT-established library of binding and dissociation energies for C–V clusters (see review in Ref. [8]). The migration energy of the 2CV complex, 1.1 eV, was deduced by fitting the model to the experimental data.

DFT calculations were performed with VASP code [12], employing the Projector Augmented Wave method [13] and parameterization established in our previous work [8], whose details and accuracy are described in supplementary material. The resulting binding energies,  $E_B$ , for C–V complexes, obtained using the standard definition (i.e. the difference in the total energy of two defects being together and apart [4]), are given Table 1. The VASP-relaxed configurations were used to compute the positron lifetime employing the DOPPLER code [14–16].

The positron lifetime,  $\tau$ , computed for a number of C–V clusters, is presented in Figure 1 together with the their lowest energy structures.  $\tau_{\text{bulk}} = 96$  ps and  $\tau_{V1} = 165$  ps correspond to the bulk Fe and a single vacancy. The excess lifetime of 70 ps for a single vacancy is in a good agreement with experimental result 65 ps ( $\tau_{\text{bulk}} = 110$  ps and  $\tau_{V1} = 175$  ps [3]). The addition of C next to a vacancy reduces  $\tau$  down to 140 ps according to our calculations, which also perfectly matches the experimental lifetime of 135 ps defined for the C–V pair [3].

The lifetime values for larger C–V complexes revealed several unexpected features. A di-vacancy in its lowest energy configuration [17] has the same lifetime as  $\tau_{V1}$ . V3 and V4 clusters form compact symmetric structures with  $\tau_{V3} = 197$  ps and  $\tau_{V4} = 202$  ps, and therefore should be clearly distinguishable from single vacancies and CV pairs in PAS.

**Table 1.** Properties of C–V complexes introduced in the KRT model.

	$E_B$ (eV)	Emitting species
C–V	0.68	V
2C–V	1.01	C
3C–V	0.29	C
V2	0.30	V
V3	0.37	V
V4	0.62	V
C–V2	0.58	V
C–V3	0.34	V
C–V4	0.37	V
2C–V2	0.31	V
3C–V2	0.78	V
4C–V2	0.91	C
	$E_M$ (eV)	$D_0, \text{m}^2 \text{s}^{-1} \text{K}^{-1}$
V	0.55	$23 \times 10^{-6}/8$
C	0.86	$1.44 \times 10^{-7}/24$
V2	0.54	$23 \times 10^{-6}/4$
V3	0.43	$23 \times 10^{-6}/4$
2CV	1.1	$1.44 \times 10^{-7}/2$

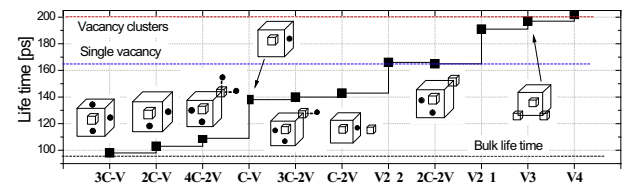


**Figure 1.** Lifetime of C–V clusters and their structures corresponding to the lowest formation enthalpy. An empty square and filled circle denote a vacancy and a C atom, respectively. Configurations marked “V2\_1” and “V2\_2” are the di-vacancies representing, respectively, first and second nearest neighbours.

The decoration of a single vacancy by C atoms progressively reduces the lifetime so that  $\tau_{3CV}$  is comparable to the Fe bulk lifetime. Hence, certain C–V clusters are “invisible” to PAS. The lifetime of the C–V complexes containing two vacancies varies from 140 up to 190 ps depending on the number of decorating C atoms so that  $\tau_{\text{bulk}} < \tau_{3CV2} < \tau_{4CV2} < \tau_{CV2} < \tau_{2CV2} \approx \tau_V = 165$  ps. Note that carbon decoration of di-vacancy restructures the arrangement of vacancies towards compact complex—see 4C–V2 in Figure 1. The lifetime of this cluster is 192 ps, i.e. essentially higher than  $\tau_V$ . The formation of NC–V2 ( $N = 1, 2, 3, 4$ ) clusters and their decay by emission of C atoms will therefore result in their detection as clustered vacancy defects. Following the lifetime calculations, the C–V clusters are subdivided into visible “single” or “clustered” vacancies to compare with the experimental spectra.

The experimental identification of clustered vacancies, in situation when  $C_C > C_V$  as observed experimentally [3], implies the formation 4CV2 and some larger C–V clusters (such as 5C–V2 or 6C–V2). Upon annealing above 450 K their formation may be realized via the decay of C–V, resulting in the formation of 2CV, which would grow to 2CV2, 3CV, 3CV2 and finally to 4CV2. However, 2CV2, 3CV and 3CV2 clusters are unstable above 450 K, while 2CV decays beyond 600 K. The

migration of the stable 2CV at  $T > 450$  resulting in the direct formation of 4CV2 and larger C–V complexes offers an alternative explanation. In fact, the migration of the 2C–V complex was found in MD simulations using DFT-derived empirical potentials [18]. We shall consider 2CV as a mobile object to model annealing of electron-irradiated Fe–C alloy.

The annealing was modelled using the kinetic rate theory method (KRT)—see application to bcc Fe [9,19]. The formation, growth and decay of C–V complexes upon annealing was performed by solving the kinetic equations. Given that electron irradiation induces a homogeneous distribution of Frenkel pairs, and the migration of point defects and C atoms is a 3-D random-walk process [10], the application of KRT to our problem is a fast and reliable solution.

C, V, V2, V3 and 2CV complexes were considered as mobile species with jump frequency  $v = K \cdot D/a_0^2$ , where  $K$  is the number of equivalent neighbouring positions,  $a_0$  is the lattice unit of bcc Fe (2.87 Å) [20], and  $D = D_0 \exp(-E_M/k_B T)$  is the diffusion coefficient, whose prefactor  $D_0$  and migration energy  $E_M$  are provided in Table 1. Multiple  $N_C$ – $V_M$  clusters (with  $N$  and  $M = 0–4$ ) are set as immobile objects. The transition rates for the formation ( $R^+$ ) and decay ( $R^-$ ) are defined as [9]:

$$R_{AB}^+ = Z_{A-B} v C_A C_B, \quad (1)$$

$$R_{AB}^- = v C_{A-B} \exp(-E_B^{A-B}/k_B T). \quad (2)$$

Here  $A$  and  $B$  represent C–V complexes with concentration  $C_{A,B}$ . The decay occurring by either emission of a vacancy or C atom is determined by the highest dissociation rate (see Eq. (2)).  $E_B$  is the binding energy of an emitted species and C–V complex.  $v$  is the jump frequency of an emitted species in Eq. (2) or of a migrating element forming  $A$ – $B$  complex in Eq. (1).  $Z_{A-B}$  is the factor accounting for the complex interaction geometry of different C–V complexes and its physical meaning is the capture radius. Following the previous study [9], we have set  $Z_{V-V} = 1$ ,  $Z_{V-C} = 10$ ,  $Z_{C-V} = 1$ , and unity was used for all other complexes.

The vacancy–dislocation reaction rate was determined as  $-pD_V C_V$  with  $p = 10^{13} \text{ m}^{-2}$  being the dislocation density expected in the annealed bcc Fe. The SIA–vacancy recombination rate was taken as  $R_{SIA-V}^+ = v_V C_I N_I C_V$ , where  $N_I$  and  $C_I$  are the mean size and concentration of SIA clusters formed upon annealing up to 200 K, following our previous study [2,10].

Two irradiation doses of  $3 \times 10^{18}$  and  $1 \times 10^{18}$  electrons  $\text{cm}^{-2}$  in Fe–C containing  $50 \times 10^{-6}$  of carbon were considered [3]. The annealing was modelled starting from the vacancy migration onset up to 600 K corresponding to the limit of the stability of 2C–V complexes. Initial concentration of SIA clusters (with multiplicity  $N_I$ ) was introduced to mimic the effect of annealing up to 200 K, resulting in SIA clustering. The input was taken from our previous kMC simulations [8]. For the low and high dose we found, respectively,  $N_I = 4$ ;  $C_{SIA} = 1$  at. ppm and  $N_I = 5$ ;  $C_{SIA} = 5$  at. ppm. Thus, the main source for the recombination of migrating vacancies are SIA clusters, since  $R_{SIA-V}^+$  is at least two orders of magnitude higher than the

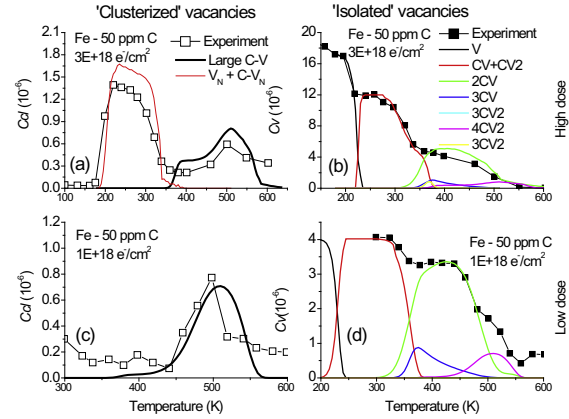


**Figure 2.** Evolution of C–V complexes upon annealing: concentration of clustered ( $Ccl$ ) and isolated ( $Cv$ ) vacancies, respectively, in (a,b) high-dose and (c,d) low-dose samples. The “Large C–V” component in (a) and (c) corresponds to 4VC2 and larger clusters. The experimental defect concentrations are obtained by decomposition of lifetime spectra measured in Ref. [3].

dislocation sink strength,  $pD_V C_V$ . At this stage, any significant contribution of dislocations to the vacancy recombination would occur at an unrealistically high dislocation density of  $\geq 10^{15} \text{ m}^{-2}$ . The recombination on the small SIA clusters, however, implies their stability at least up to the vacancy migration stage. Even though MD simulations suggest that di-, tri- and four-SIA clusters migrate below 200 K [21,22], DFT calculations have revealed “non-parallel” SIA configurations [23] with much higher activation energy than canonical SIA platelets [10]. Activation-relaxation techniques have proven that the migration of non-parallel  $I_3$  may require an activation energy of up to 1.2 eV [24]. SIA clusters are therefore considered as immobile objects at least up to the onset of 2CV migration. Then the concentration of SIA clusters drastically drops (due to V–SIA recombination) and dislocations act as major sinks.

The evolution of isolated vacancies and the C–V complexes is shown in Figure 2b,d. At  $\sim 220$  K, a substantial concentration of CV and CV2 clusters is formed once vacancies become mobile. The dissociation of these complexes occurs around 300 K, close to the stage of interstitial carbon migration. Some vacancies annihilate with SIA clusters, some contribute to the formation of 2CV clusters, and a certain concentration of “invisible” 3CV clusters is also established. Above 350 K, all visible vacancies are stored in 2CV and 3CV clusters. Beyond  $\sim 380$  K, 3CV clusters begin to emit C atoms.

As temperature increases further, the migration of 2CV results in the formation of 4CV2 and larger C–V clusters, contributing to the “clustered vacancy” signal. Therefore, the density of the “large C–V” clusters and pure vacancy clusters is compared in Figure 2a,c with the PAS signal attributed to the clustered vacancies. The best agreement for the positions and intensities of clustered vacancies ( $Ccl$ ) with the experimental results was found using  $E_M(2CV) = 1.1$  eV. The decay of the 4CV2 clusters, which is a first-order reaction, begins at about 550 K with an activation energy of 1.8 eV.

Emitted C and V reform as 2C–V complexes, which are by 0.1 eV more stable than 4CV2. Finally, 2CV dissociate and relieved vacancies recombine on dislocations.

The presented KRT model was also applied to reveal the most influential inputs determining a principal agreement with the experimental data. We found that correct density of clusterized vacancies at 200–300 K is achieved only if the trapping of V2 and V3 clusters at C atoms is taken into account. Exclusion of the CV, CV2 and CV3 formation does not return an acceptable shape of the *Ccl* signal and the fraction of recombined vacancies is too high. A good agreement for the evolution of isolated vacancies (*Cv*) at  $T = 300\text{--}450$  K cannot be achieved unless SIA clusters with the concentration of  $\geq 1$  at. ppm are present, as the sink strength of dislocations is too small (see discussion in Ref. [8]). This implies that SIA cluster growth ceases at sizes 4–6, consistent with the low mobility of “non-parallel” clusters [23,24]. Finally, the assumption on the mobility of 2CV and on the presence of stable SIA clusters (up to 450 K) is necessary to get quantitative agreement for *Ccl* at  $T > 450$  K. In the absence of the numerous small SIA clusters, the calculated intensity of *Ccl* is higher than the experimental one by a factor of five.

To conclude, using a combined ab initio and kinetic rate theory study we have analyzed positron lifetime spectra in irradiated Fe–C upon thermal annealing up to 600 K. The assessment reveals three principal findings on the properties of point defects in Fe–C system: (i) the migration of small SIA clusters ( $I_4\text{--}I_6$ ) formed after the recovery stage II (150–180 K) is  $> 1.2$  eV, possibly due to stabilization by C atoms; (ii) the migration energy of 2CV clusters is  $\sim 1.1$  eV, while its dissociation energy is  $\sim 1.9$  eV; and (iii) the mobility of the 2CV complexes is a principal component providing vacancy clustering upon annealing at 450–600 K in agreement with experiment.

Here, we did not account for the vibrational entropy contribution to the free formation and migration energies. This contribution was evaluated by Forst et al. [5] to be  $\sim 0.2$  eV for some of C–V complexes considered here. Even though it is an important correction, it does not change the two principal conclusions about mobility of the 2CV complex and the abnormally high migration energy of  $I_3\text{--}I_6$  clusters.

This work, supported by the European Communities, was carried out within the framework of EFDA/EURO fusion.

- [1] S.J. Zinkle, J.T. Busby, *Mater. Today* 12 (2009) 12.
- [2] S. Takaki, J. Fuss, H. Kugler, U. Dedek, H. Schultz, *Radiation Eff.* 79 (1983) 87.
- [3] A. Vehanen, P. Hautojärvi, J. Johansson, J. Yli-Kauppila, *Phys. Rev. B* 25 (1982) 762.
- [4] C. Domain, C. Becquart, J. Foct, *Phys. Rev. B* 69 (2004) 144112.
- [5] C.J. Forst, J. Slycke, K.J. Van Vliet, S. Yip, *Phys. Rev. Lett.* 96 (2006) 175501.
- [6] T.T. Lau, C.J. Forst, X. Lin, J.D. Gale, S. Yip, K.J. Van Vliet, *Phys. Rev. Lett.* 98 (2007) 215501.
- [7] C.C. Fu, E. Meslin, A. Barbu, F. Willaime, V. Oison, *Solid State Phenom.* 139 (2008) 157.
- [8] D. Terentyev, G. Bonny, A. Bakaev, D. Van Neck, *J. Phys.: Condens. Matter* 24 (2012).
- [9] K. Tapasa, A. Barashev, D. Bacon, Y. Osetsky, *Acta Mater.* 55 (2007) 1.
- [10] C. Fu, J. Dalla Torre, F. Willaime, J. Bocquet, A. Barbu, *Nat. Mater.* 4 (2005) 68.
- [11] M.J. Puska, R.M. Nieminen, *J. Phys. F: Met. Phys.* 12 (1982) L211.
- [12] M.R. Press, S.N. Khanna, P. Jena, M.J. Puska, *Z. Phys. B: Condens. Matter* 81 (1990) 281.
- [13] M. Eldrup, B.N. Singh, S.J. Zinkle, T.S. Byun, K. Farrell, *J. Nucl. Mater.* 307–311 (2002) 912.
- [14] Y. Nagai, K. Takadate, Z. Tang, H. Ohkubo, H. Sunaga, H. Takizawa, M. Hasegawa, *Phys. Rev. B* 67 (2003) 224202.
- [15] G. Kresse, J. Hafner, *Phys. Rev. B* 47 (1993) 558.
- [16] G. Kresse, D. Joubert, *Phys. Rev. B* 59 (1999) 1758.
- [17] C. Domain, C. Becquart, *Phys. Rev. B* 65 (2002) 024103.
- [18] D. Terentyev, N. Anento, A. Serra, V. Jansson, H. Khater, G. Bonny, *J. Nucl. Mater.* 408 (2011) 272.
- [19] A. Barbu, E. Clouet, *Solid State Phenom.* 129 (2007) 51.
- [20] C. Kittel, *Introduction to Solid State Physics*, John Wiley and Sons, New York, 1987.
- [21] D. Terentyev, L. Malerba, M. Hou, *Phys. Rev. B* 74 (2007) 104108.
- [22] N. Anento, A. Serra, Y.N. Osetsky, *Model. Simul. Mater. Sci. Eng.* 18 (2010) 025008.
- [23] D. Terentyev, T. Klaver, P. Olsson, M. Marinica, F. Willaime, C. Domain, L. Malerba, *Phys. Rev. Lett.* 100 (2008) 145503.
- [24] M.-C. Marinica, F. Willaime, N. Mousseau, *Phys. Rev. B* 83 (2011) 094119.